IPS Journal of Molecular Docking Simulations
IPS J Mol Dock Sim., 3(1): 58-70 (2025)
DOI: https://doi.org/10.54117/ijmds.v3i1.42

In vitro and *In silico* Studies of *Plumbago zeylanica* Root Fractions on Mitochondrial-Related Parameters on Male Wistar Rats

Joshua Gbadebo Ojo, Patience Folashade Olabinri, Ayobami Damilare Adisa, Leonard Ona Ehigie, Adeola Folasade Ehigie*

Department of Biochemistry, Ladoke Akintola University of Technology, Ogbomoso, Nigeria.
*Corresponding author e-mail: afehigie@lautech.edu.ng

Abstract

The mitochondrial permeability transition pore (mPTP) controls release of pro-apoptotic factors; its modulation is a therapeutic strategy for diseases characterized by dysregulated apoptosis. This study evaluated the effects of *Plumbago zeylanica* (PZ) root fractions on mitochondrial function in male Wistar rat liver and investigated molecular interactions between key phytochemicals and Cyclophilin D (CypD), a regulator protein of mPTP. Aqueous root extract was partitioned into hexane, ethyl acetate, butanol, and residual aqueous fractions. Isolated rat liver mitochondria were incubated with graded concentrations (4–20 µg/mL) of each fraction. mPTP opening was monitored spectrophotometrically at 540 nm (mitochondrial swelling assay). Mitochondrial ATPase activity and lipid peroxidation (TBARS) were measured. Phytochemical composition was profiled by HPLC/GC-FID. Selected phytochemicals were docked to human CypD using AutoDock Vina; chitranone (top hit) underwent 50 ns molecular dynamics (GROMACS). All organic fractions induced significant mPTP opening in a concentration-dependent manner (maximum fold inductions at 20 µg/mL: BRF 9.7-fold; HRF 9.4-fold; ARF 9.4-fold; ERF 9.1-fold; spermine reversed pore opening). Mitochondrial ATPase activity increased significantly ($p<0.05$). Lipid peroxidation inhibitory capacity decreased compared to control ($p<0.05$). HPLC/GC identified plumbagin and chloroplumbagin as major peaks. Docking showed stable interactions between phytochemicals and CypD; chitranone exhibited the highest binding affinity (−8.5 kcal·mol^{-1}) and formed three hydrogen bonds with Asp227, Asn141 and Gly222. MD trajectories indicated stable ligand–protein complexes. PZ root fractions modulate mPTP opening and mitochondrial function *in vitro*, and chitranone displays favourable binding to Cyclophilin D *in silico*. These data suggested a mitochondrial-mediated mechanism underlying the cytotoxic properties of PZ. Further *in vitro* and *in vivo* studies are required.

Keywords: *Plumbago zeylanica; Chitranone; Cyclophilin D; Molecular Simulation; Mitochondrial swelling; ATPase; lipid peroxidation.*

Article History

Received: 13 Feb 2025
Accepted: 25 Sept 2025
Published: 27 Oct 2025

How to cite this paper: Ojo, J. G., Olabinri , P. F., Adisa , A. D., Ehigie, L. O., & Ehigie, A. F. (2025). In vitro and In silico Studies of Plumbago zeylanica Root Fractions on Mitochondrial-Related Parameters on Male Wistar Rats. *IPS Journal of Molecular Docking Simulations*, *3*(1), 58–70. https://doi.org/10.54117/ijmds.v3i1.42

1. Introduction

The mitochondrial permeability transition pore (mPTP) is a multiprotein complex whose opening can be triggered by a variety of cellular insults, including oxidative stress, mitochondrial calcium overload, and depletion of ATP (Verma *et al.*, 2022). The induction of mPTP opening results in the loss of mitochondrial membrane integrity, followed by the release of pro-apoptotic factors such as cytochrome c, ultimately culminating in apoptotic cell death (Bonora *et al.*, 2021). Dysregulated mPTP activity has been closely linked to the pathogenesis of several human diseases, including ischemia–reperfusion injury, neurodegenerative disorders, cardiovascular complications, and metabolic syndromes (Wang *et al.*, 2021). Given its central role in regulating cell fate, the mPTP has emerged as a critical therapeutic target in efforts to design novel strategies for disease management (Halestrap, 2009).

Pharmacological modulation of the mPTP has attracted significant attention in recent years. Several naturally derived compounds and plant fractions have been shown to influence mPTP dynamics, thereby preventing its aberrant opening and enhancing cell survival (Zhang *et al.*, 2019). These bioactive molecules act through diverse mechanisms, ranging from direct interaction with mPTP components to the modulation of upstream signaling pathways such as oxidative stress responses and calcium homeostasis (Wacquier *et al.*, 2020). The molecular regulation of mPTP involves several key proteins, including voltage-dependent anion channels (VDACs), adenine nucleotide translocator (ANT), and

cyclophilin D (CypD), all of which participate in maintaining mitochondrial calcium balance, metabolic flux, and redox stability The intricate regulation of these components underscores the importance of mPTP as a finely tuned gatekeeper of cellular life and death (Wacquier *et al*., 2020).
Natural products remain an indispensable source of therapeutic agents, particularly in oncology, where many frontline chemotherapeutics are derived from plants (Sharifi-Rad *et al*., 2019). Plant-derived compounds with strong pro-apoptotic activities are currently under extensive investigation for their potential role in cancer prevention and therapy (Sauter *et al*., 2020). Their historical use in traditional medicine further supports their pharmacological relevance, as several plant fractions have been reported to trigger apoptosis in diverse cancer cell models (Rajabi *et al*., 2021).

Plumbago zeylanica, a medicinal plant with deep roots in traditional healing practices, has emerged as a promising candidate in this regard (Shukla *et al*., 2021). The roots of *P. zeylanica* contain plumbagin, a naphthoquinone derivative, which has been widely reported for its potent anticancer activities. Chauhan *et al*. (2014) demonstrated that plumbagin exerts strong cytotoxic effects by inducing apoptosis across multiple cancer cell types. More recently, Guguloth *et al*. (2023) revealed that the methanol fraction of *P. zeylanica* roots displayed significant anticancer activity against breast and colon cancer cells through the activation of apoptotic pathways. These findings reinforce the potential of *P. zeylanica* as a natural source of bioactive compounds for cancer therapeutics.

Beyond its anticancer properties, *P. zeylanica* has been associated with a wide spectrum of pharmacological benefits, including anti-inflammatory, analgesic, antidiabetic, antimicrobial, and neuroprotective effects (Shukla *et al*., 2021; Gupta *et al*., 2021). Its neuroprotective potential, in particular, has led to its consideration as a candidate for managing neurodegenerative disorders such as Alzheimer's disease, Parkinson's disease amongst other disorders (Ittiyavirah & Ruby, 2014).

2. Materials and Method

2.1 Materials and Reagents
Distilled water, $CuSO_4.5H_2O$, NaOH, Ammonium hydroxide, phosphate buffered saline (PBS), Trypan blue 0.4 percent (Gibco, New York, USA), and other analytical grade chemicals and reagents. Filter paper, conical flask, beakers, reagent bottles, homogenizer flasks, spectrophotometer, cuvette, magnetic stirrer, stopwatch, stopwatch, dissection set.

2.2 Plant Material
PZ root was bought from Oja Jagun, Ogbomoso, Oyo State. This was identified and authenticated in the Department of Plant Biology, University of Ilorin, Ilorin, with voucher number UTLH/001/1374 was obtained.

2.3 Preparation of the crude aqueous fraction of *Plumbago zeylanica*
The preparation of *Plumbago zeylanica* roots was done according to the method described by Agbaje and Adeniran (2009) with slight modifications. The fresh roots of *Plumbago zeylenica* was washed with distilled water, drained and air-dried for 1hr. A known weight of chopped bits (500g) of the air-dried *Plumbago zeylanica* was macerated in 5000ml distilled water for 24hrs. The macerated mixture was filtered using filter paper.

2.4 Fractionation of the aqueous fraction of *Plumbago zeylanica* with organic solvents
The crude aqueous fraction of *P. zeylanica* was mixed with various organic solvents (n-hexane, ethylacetate, butanol, and water) for 1 hr and separated using a separating funnel to obtain the Hexane, Ethylacetate, Butanol, and Aqueous fractions respectively. The separated organic portions were concentrated using rotary evaporator at 50°C and weighed to calculate the percentage yield.

2.5 Experimental animals and ethical approval
Twenty male Wistar rats weighing between 100 g and 150 g were used for the experiment. The animals were purchased from the animal house of Biochemistry department, Ladoke Akintola University of Technology and they were acclimatized for a period of two weeks. Ethical clearance was given by the faculty of basic medical sciences, Ladoke Akintola University of Technology.

2.6 Phytochemical Screening
2.6.1 Test for glycosides: The extract was hydrolysed by hydrochloric acid for a few hrs on a water bath. Then 1ml of pyrimidine and a few drops of sodium nitroprusside solutions were added to the solution. Then it was made alkaline by adding sodium hydroxide solution. Appearance of pink to red colour showed the presence of glycosides.

2.6.2 Detection of phenols: Presence of phenols was detected by ferric chloride test. Extract was treated with 3 – 4 drops of ferric chloride solution. Formation of bluish black colour indicate the presence of phenols.

2.6.3 Test for steroids: 1ml of the extract was dissolved in 10ml of chloroform and equal volume of concentrated sulphuric acid was added by sides of the test-tube. Formation of yellow with green fluorescence colour indicates the presence of steroids.

2.6.4 Test for emodins: 2ml of 10% NH_4OH and 3ml of benzene was added to the extract. Appearance of red colour indicates the emodins.

2.6.5 Test for coumarins: 3ml of 10% NaOH was added to 2ml of extract. Formation of yellow colour indicates the presence of coumarins.

2.6.6 Test for fatty acids: 0.5ml of extract was mixed with 5ml of ether. These extracts were allowed for evaporation on filter paper and dried the filter paper. The appearance of transparency on filter paper indicate the presence of fatty acids.

2.6.7 Test for proteins: The extract was treated with drops of concentrate nitric acid. Formation of colour indicates the presence of proteins.

2.6.8 Test for carbohydrates: Extract was dissolved in 5ml distilled water and filtered. The filtrate was treated with 2 drops of alcoholic alpha-naphthol solution in a test-tube. Formation of a violent at the junction indicated the presence of carbohydrates.

2.6.9 Test for flavonoids: 1ml of extract was taken in a test tube and a few drops of dilute sodium hydroxide were added. An intensive yellow colour is produced and become colourless on addition of few drops of dilute HCl which indicates the presence of flavonoids.

2.6.10 Test for alkaloids: Extract (0.5g) was diluted to 10ml with acid alcohol then boiled and filtered. 2ml of dilute 10% ammonia was added to 5ml of the filtrate. Then 5ml of chloroform was added to this content and shaken gently. The chloroform layer was extracted with 10ml of acetic acid which was divided into two portions. Mayer's reagent was added to one portion and Draggendorf's reagent to the other. The formation of cream with Mayer's reagent or reddish brown.

2.6.11 Test for Tannins: about 0.5g of the extract was boiled in 10ml of water in a test tube and then filtered. Few drops of 0.1ml of water in a test tube and filtered. Few drops of 0.1% ferric chloride was added and observed for brownish green or blue-black colouration which indicates the presence of tannins.

2.6.12 Test for saponins: Extract (0.5g) was taken in a test tube and 5ml of distilled water was added. This mixture was shaken vigorously and observed for a stable persistent froth. That froth was mixed with 3 drops of Olive Oil and shaken vigorously. The formation of an emulsion indicates the presence of saponins.

2.7 Isolation of rat liver mitochondria

The liver was excised from the rats and washed in a buffer solution. The liver was then homogenized, and the homogenate was centrifuged to obtain the mitochondrial fraction. The mitochondrial pellets were washed and suspended in buffer for further experiments.

2.8 Mitochondria swelling assay

Mitochondrial permeability transition was determined according to the method of Lapidus and Sokolove (1994). Using a Spectrum lab 752ns UV/Visible spectrophotometer, variations in the absorbance of mitochondria at 540 nm in the presence and absence of calcium ions (a triggering agent) were measured over a period of twelve mins and the changes in absorbance were recorded over time.

2.9 Determination of ATPase activity

Mitochondrial ATPase activity was assessed using Lardy and Wellman (1953) method. The mitochondrial protein samples were incubated with ATP, and the reaction was allowed to proceed. The reaction was stopped, and the resulting solution was used to measure colour development.

2.10 Determination of percentage inhibition of lipid peroxidation

The extent of lipid peroxide formed was measured by using low ionic strength mitochondrion as a lipid-rich medium according to modified methods of Ruberto *et al*. (2000). Briefly, 0.5 mL of mitochondria suspension and varying concentrations of root fractions of *Plumbago zeylanica* were added to test tubes and made up to 1 mL with distilled water. Lipid peroxidation was induced by the addition of ferrous sulfate (0.07 mmol/L). Furthermore, acetic acid (20%), thiobarbituric acid (TBA, 0.8%), and sodium dodecyl sulfate (SDS, 1.1%) were added to the solution. The mixture was vortexed and heated at 95º C for 60 min. After cooling the absorbance was measured at 532 nm. All experiments were carried out in triplicates.

2.11 Molecular docking and Molecular simulation

Molecular docking and molecular simulation studies were conducted using Autodock Vina and GROMACS, respectively. Autodock Vina was used for virtual screening and analyzing binding affinities, while GROMACS was used for molecular dynamics simulations.

2.12 Statistical Analysis

The results were analyzed using one-way ANOVA followed by Dunnett's test. The data are presented as mean ± standard error of the mean. GraphPad Prism 6 and Microsoft Excel 2013 were used for statistical analyses.

3. Results

3.1 Phytochemical Screening

Table 1 showed the phytochemical analysis of *PZ* indicated the existence of alkaloids, anthraquinones, steroids, phenolic compounds, terpenoids, tannins, phlobatannins, saponins, glycosides, and proteins.

Figure 1 and 2 showed GC-FID and HPLC analyses unveiled plumbagin and chloroplumbagin as the components exhibiting the highest peak values.

3.2 *in vitro* opening of MMPT pore by *PZ*

Figure 3A showed the effect of Ca^{2+} and spermine on the isolated mitochondria of normal rats by incubating with calcium for 3 mins. This showed MMPT pore opening by 11.2 folds and it was reversed by spermine. Figure 3B, C, D and E showed *in vitro* induction of MMPT pore opening by changes in absorbance after the addition of varying concentrations of ERF, HRF, ARF and BRF respectively for a period of 12 mins in the absence of calcium (triggering agent). After exposing the mitochondria to varying concentrations (4, 8, 12, 16 and 20 µg/mL) of ERF, HRF, ARF and BRF. MMPT pore opening was triggered by 5.0, 3.1, 5.3, 5.6 and 9.1, folds for ethylacetate root fraction (ERF); 5.3, 5.0, 5.6, 9.1 and 9.4 folds for n-Hexane root fraction (HRF); 3.3, 5.0, 5.4, 6.4 and 9.4 folds for Aqueous root fraction (ARF) and 4.4, 5.9, 7.8, 9.1 and 9.7 folds for Butanol root fraction (BRF) folds respectively. The observed pore opening was inhibited by spermine (a standard inhibitor of the pore).

3.3 *in vitro* mitochondrial ATPase

Mitochondrial ATPase activity (as shown in Figure 4) was notably heightened in the groups tested with *PZ* root fraction compared to the control group.

3.4 Percentage inhibition of lipid peroxidation

The results obtained in Figure 5 showed decreased levels of percentage inhibition of lipid peroxidation when compared with control group.

3.5 Molecular Docking and Simulation

Figures 6 A and B shows the results of a molecular docking where two compounds were tested to see how well they bind together. The first compound, referred to as the "Chitranone" (ligand) showed a binding affinity of -8.5 and formed 3 hydrogen bonds at specific amino acid positions (Asp 227, Asn141, Gly 222). The second compound, known as the "Emodin" (standard), had a binding affinity of -7.0 and formed hydrogen bonds at different amino acid positions (Arg 179, Glu 177). Even though both compounds had the same number of hydrogen bonds, the chitranone showed a better affinity for binding. This suggests that the chitranone may be more effective or efficient in its interactions compared to the standard compound.

The radius of gyration serves as an indicator of the dimensions and density of a molecule. When comparing chitranone and emodin, it was observed that the radius of gyration was lower for chitranone than for emodin, as illustrated in figure 7A. This suggests that chitranone possesses a more condensed molecular structure than emodin, possibly attributed to the existence of a cyclopentane ring within its chemical composition.

Root Mean Square Deviation (RMSD) served as a metric for assessing the positional disparity between two structures. It quantified the mean distance between the atomic positions within a molecule at different time points in relation to a designated reference structure. This measurement offers insights into the overall stability and structural alterations of the molecules under study. Notably, the RMSD value for chitranone is observed to be lower than that of emodin, indicating that the binding orientation of chitranone closely resembles that of the native ligand, as depicted in Figure 7B.

The Root Mean Square Fluctuation (RMSF) serves as a metric for gauging the movement of the ligand or protein, offering insights into the flexibility and mobility of specific regions within the molecule. In Figure 8A, the RMSF of chitranone registers lower compared to that of emodin, indicating that chitranone exhibits greater stability and is less prone to movement during the simulation.

Hydrogen bonding stands as a crucial force in biological systems, playing a significant role in the binding of a ligand to a protein, in the case of chitranone, simulation outcomes suggest the presence of several hydrogen bonding interactions between the ligand and the proteins, such as those between chitranone and glycine, as well as chitranone and aspartic acid. These hydrogen bonds between chitranone and the protein are visually represented in Figure 8B.

This study demonstrated that PZ root fractions promote mPTP opening, increase ATPase activity, and reduce antioxidant protection in vitro. Docking and MD analyses implicate interactions of phytochemicals such as chitranone with Cyclophilin D, supporting a mitochondrial-mediated mechanism of apoptosis. Increased ATPase activity and reduced TBARS inhibition reflect mitochondrial dysfunction and oxidative stress.

Table 1: Results of phytochemical screening of total fraction of *PZ*

TEST	PZ *Ethylacetate Result*	PZ *Butanol Result*	PZ *N-Hexane Result*	PZ *Aqueous Result*
Flavonoid	–	+++	–	+++
Protein	+++	–	++	–
Coumarins	–	–	–	–
Steroid	–	–	+++	–
Phenol	+++	+++	+++	+++
Saponins	+++	+++	+++	+++
Tannin	+++	+++	+++	+++
Terpenoids	+	+++	+++	+
Anthraquinones	-	+	-	+
Alkaloids	-	-	+	-
Phlobatannins	+	+	+	+
Carbohydrates	-	-	-	-

Note: +++, *high concentration;* ++, *medium concentration;* –, *nil.*

Temperature Program:

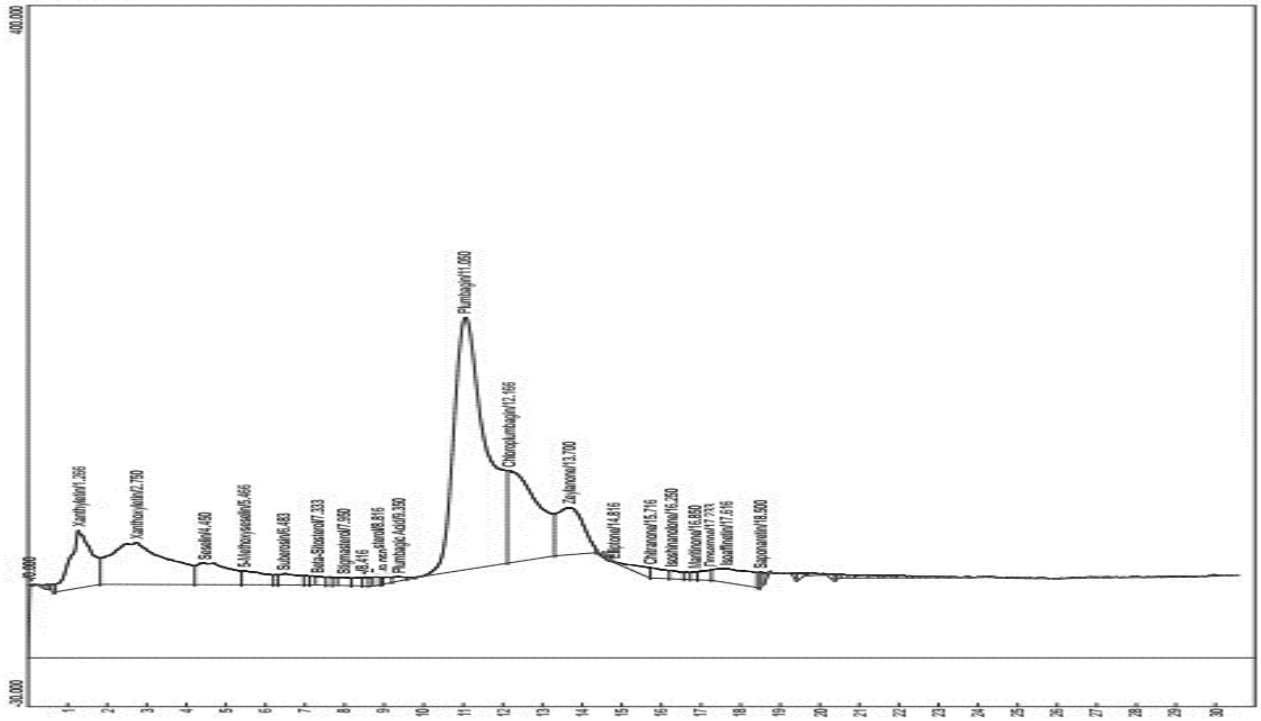

Figure 1. Butanol root fraction of *Plumbago zeylanica* phytochemicals by HPLC.

Temperature program:

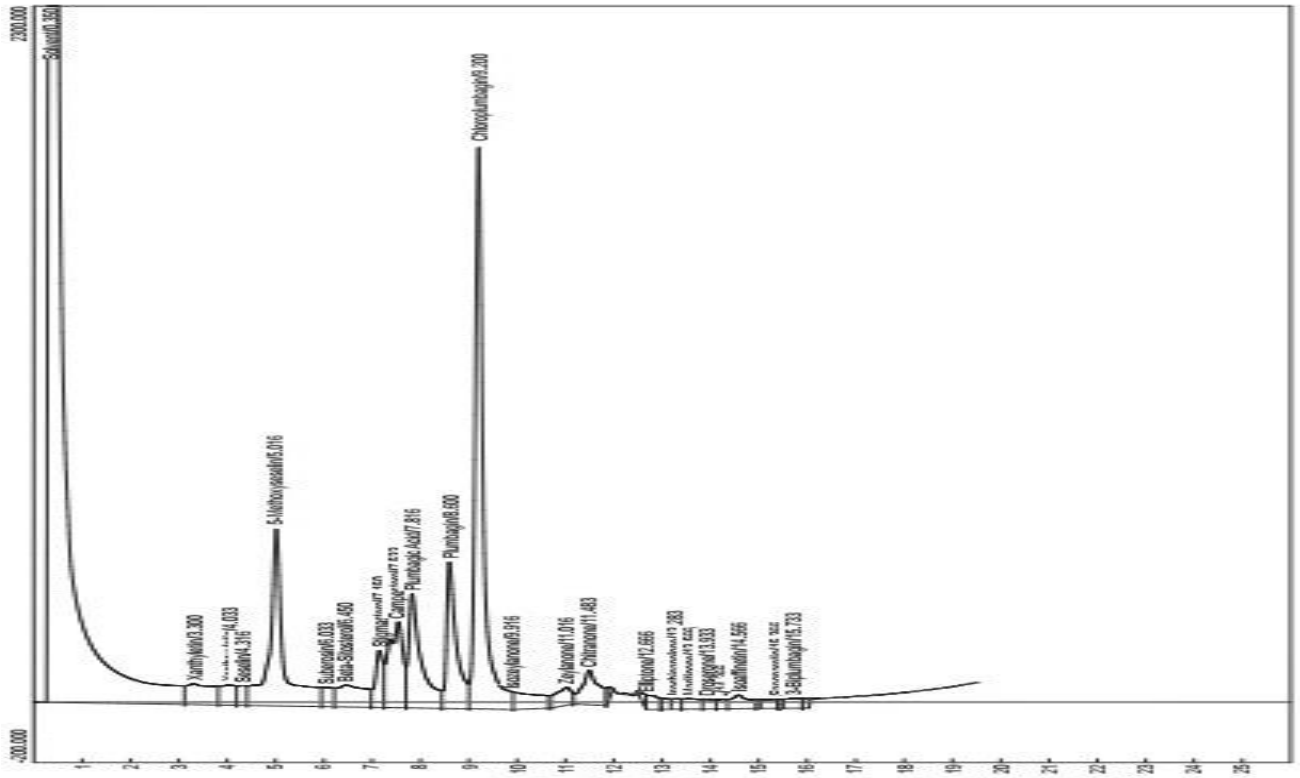

Figure 2 Butanol root fraction of *Plumbago zeylanica* phytochemicals by GC-FID.

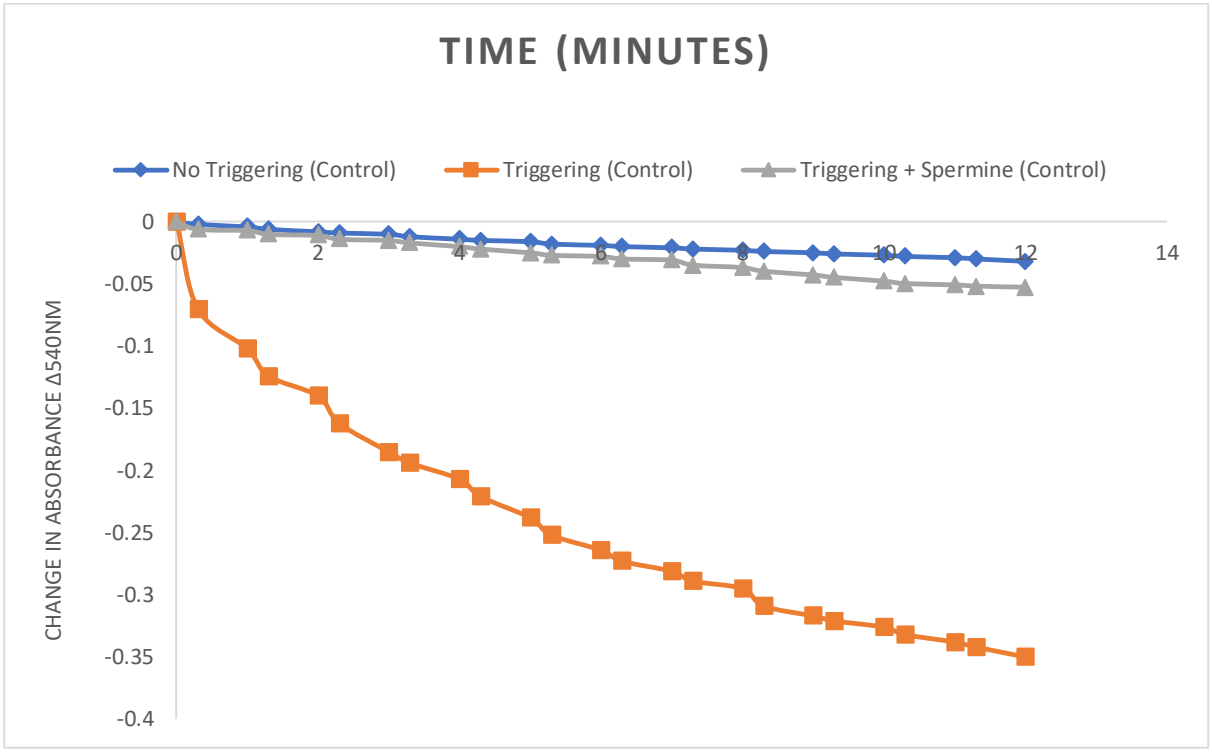

Figure 3A: *In-vitro* inductive effect of triggering agent (Ca^{2+}) on mitochondrial membrane permeability transition pore and reversal with spermine.

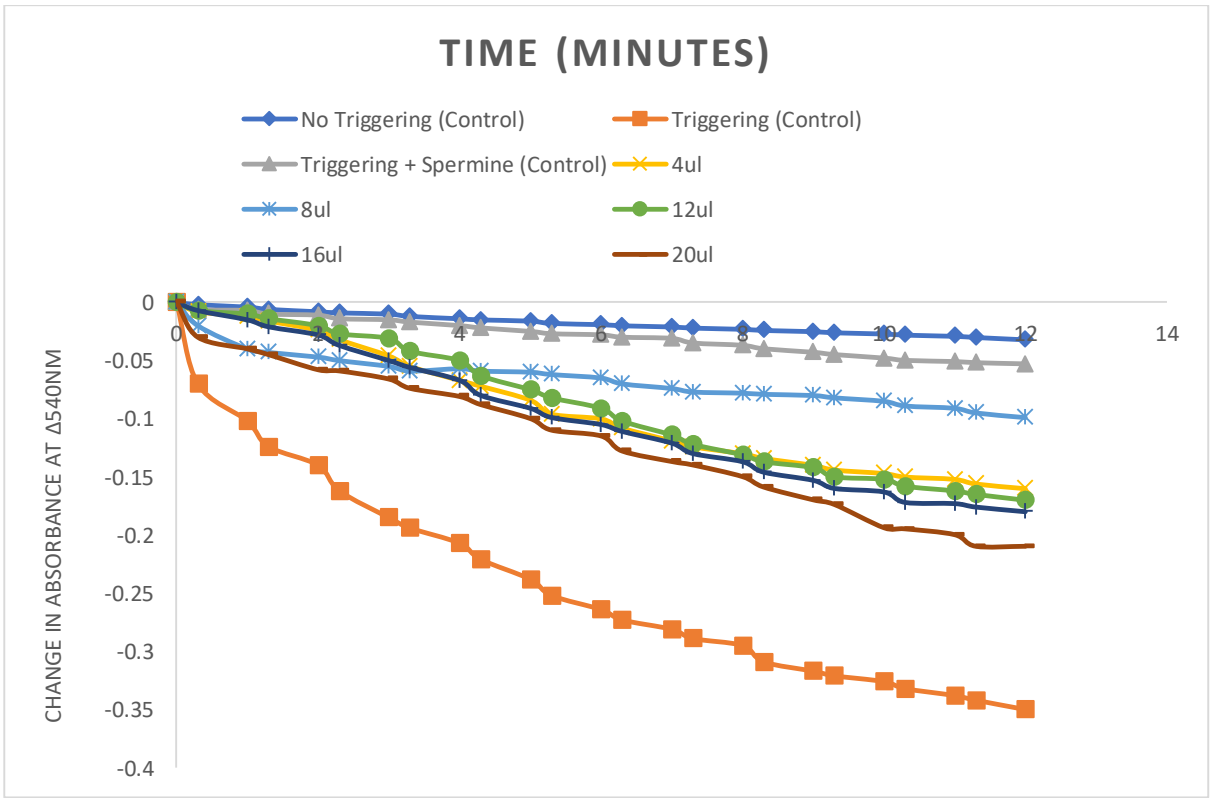

Figure 3B: *In vitro* induction of rat liver MMPT pore opening by varying concentrations of root ethylacetate fraction of *Plumbago zeylanica.*

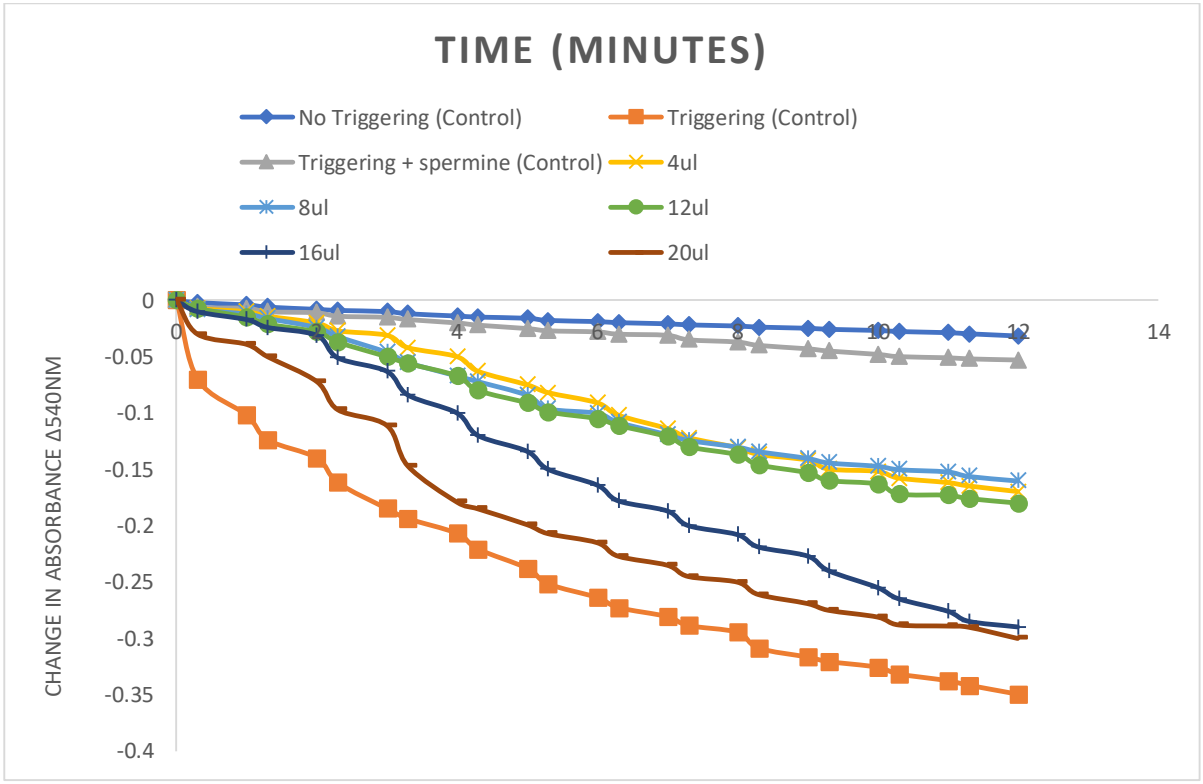

Figure 3C: *In vitro* induction of rat liver MMPT pore opening by varying concentrations of root n-Hexane fraction of *Plumbago zeylanica*.

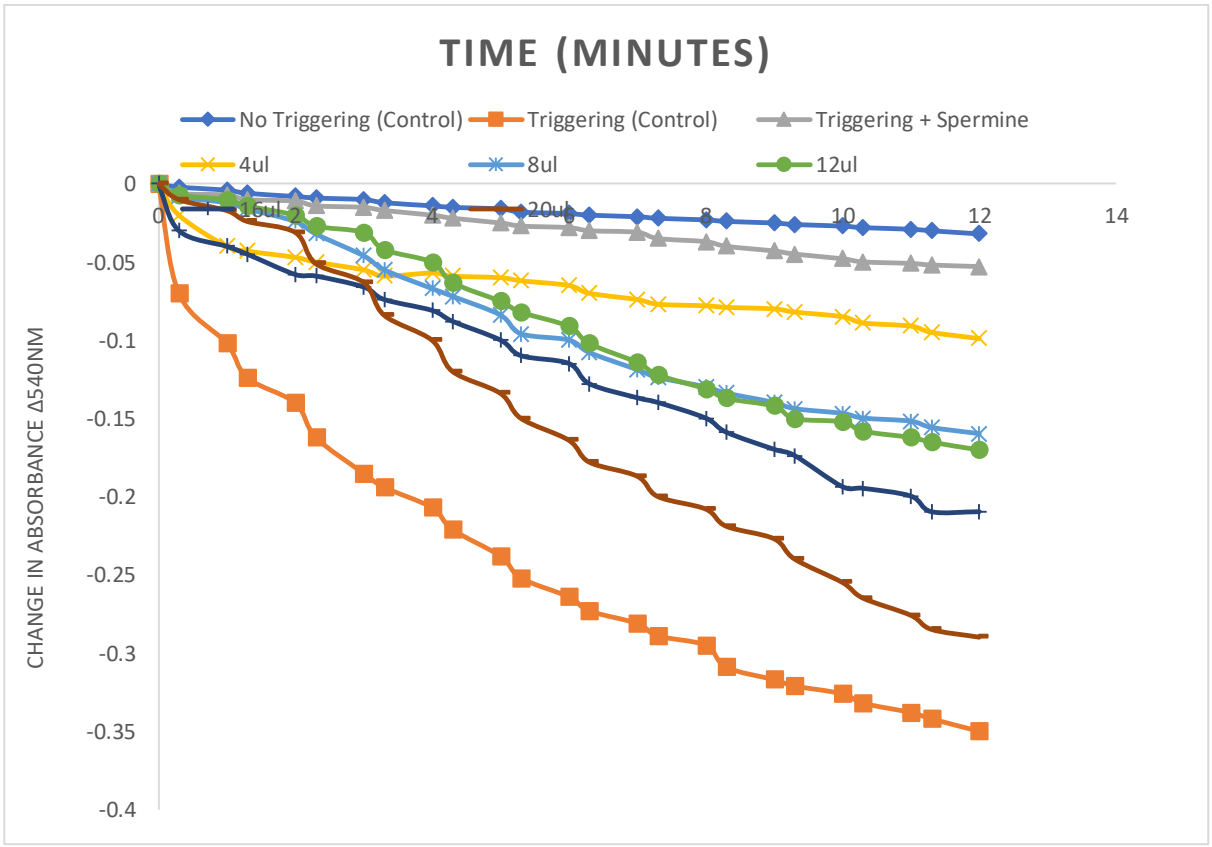

Figure 3D: *In vitro* induction of rat liver MMPT pore opening by varying concentrations of root aqueous fraction of *Plumbago zeylanica*.

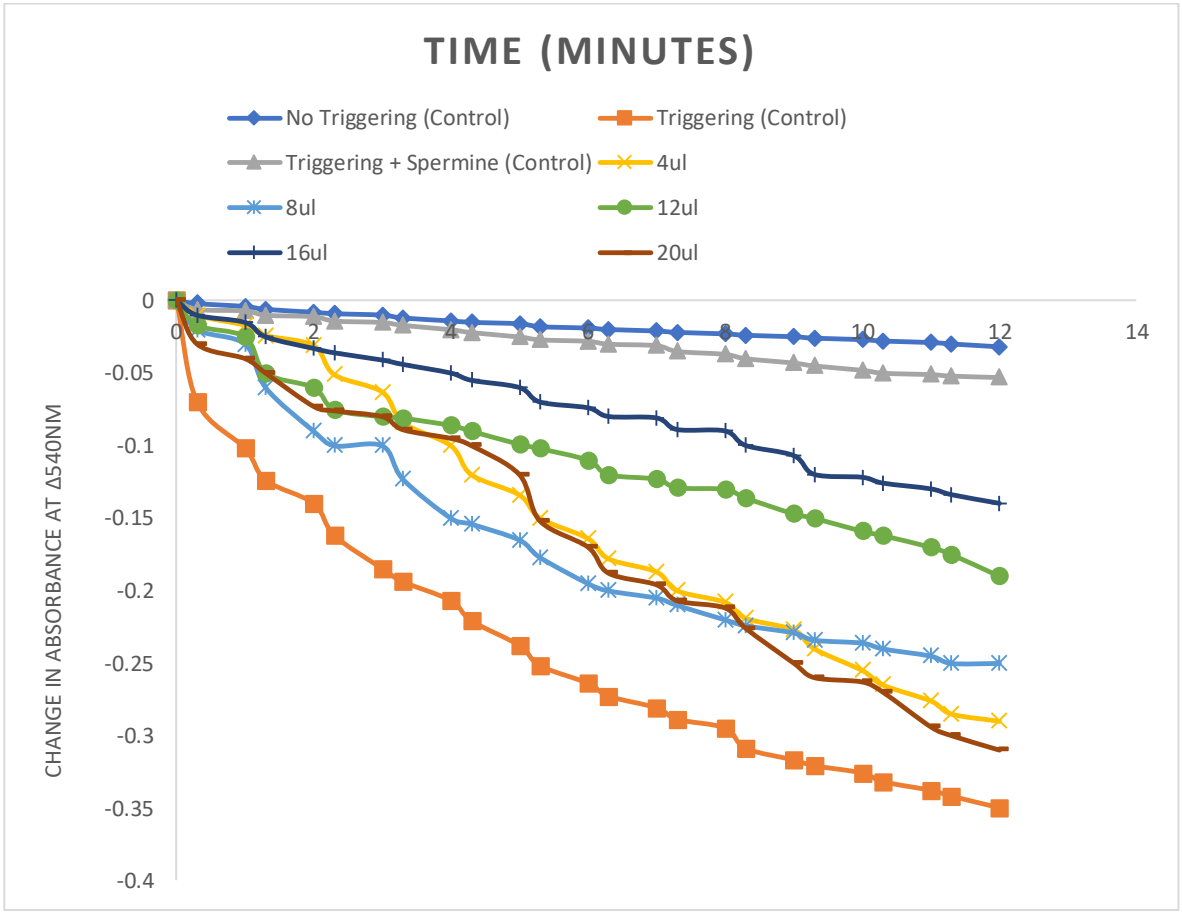

Figure 3E: *In vitro* induction of rat liver MMPT pore opening by varying concentrations of root Butanol fraction of *Plumbago zeylanica*.

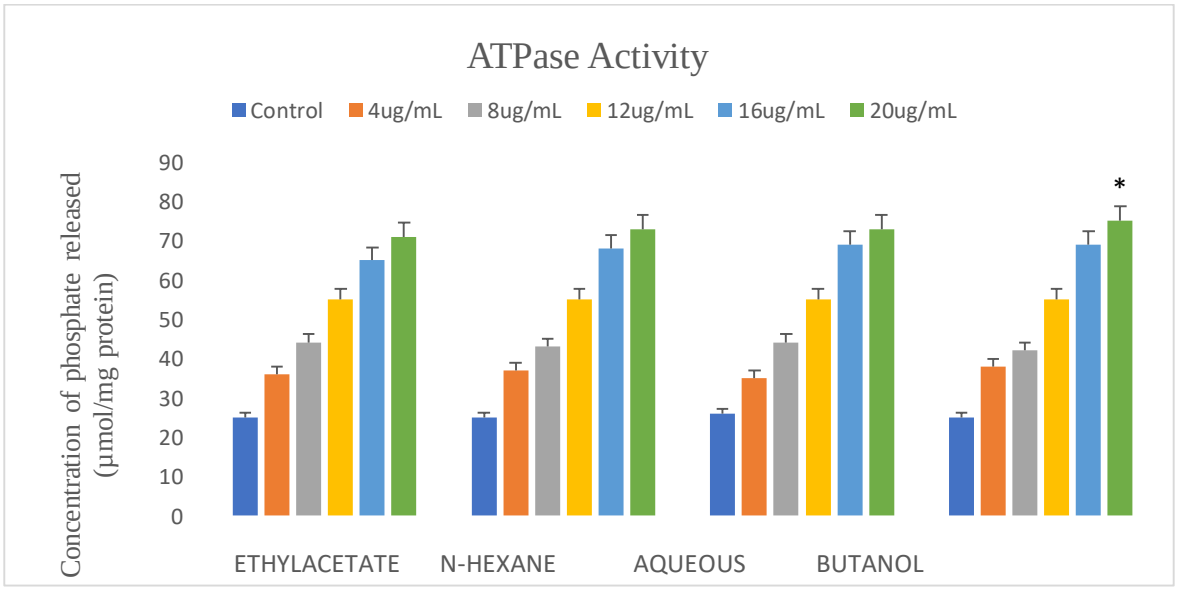

Figure 4: *In vitro* induction of normal rat ATP hydrolysis by mitochondrial ATPase activity by varying concentrations of roots fractions of *Plumbago zeylanica* (mean ± SEM, n = 6, P<0.005) vs control group.

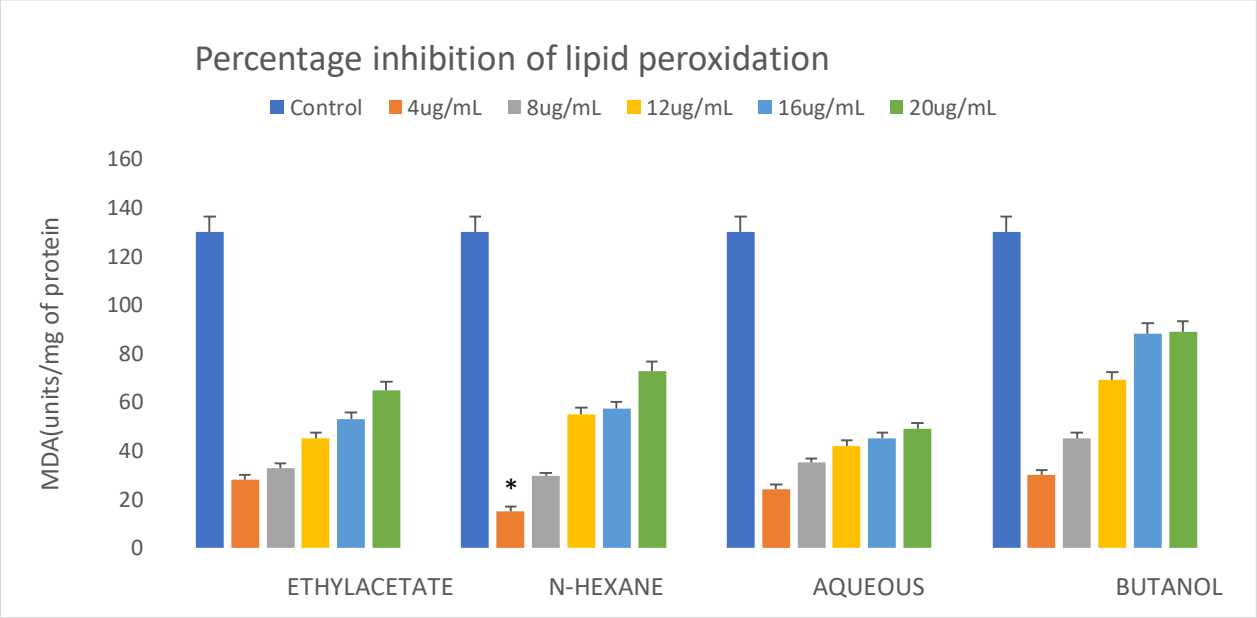

Figure 5: *In vitro* induction of normal rat percentage inhibition of lipid peroxidation by varying concentrations of roots fractions of *Plumbago zeylanica* (mean ± SEM, n = 6, P<0.005) vs control group.

Table 2: Docking Result Showing the Ligand Binding Affinity With Cyclophilin D

Ligands	*Binding Affinity*	*Hydrogen bond*	*RO5(Lipinski rule)*
Xanthyletin	-6.6	1	Accepted
Xanthoxyletin	-6.3	1	Accepted
Seselin	-6.8	1	Accepted
5-methoxyseselin	-6.7	1	Accepted
Suberosin	-6.6	1	Accepted
Beta-sitosterol	-7.0	1	Accepted
Stigmasterol	-7.5	1	Accepted
Campsterol	-7.2	2	Accepted
Plumbagic Acid	None	-	Accepted
Plumbagin	None	-	Accepted
Chloroplumbagin	-6.0	1	Accepted
Zeylanone	-7.9	1	Accepted
Elliptone	-7.1	2	Accepted
Chitranone	-8.5	3	Accepted
Isoshinanolone	-5.7	3	Accepted
Maritinone	-7.9	3	Accepted
Droserone	-6.1	3	Accepted
Isoaffinetin	-7.0	7	accepted
Saponaretin	-7.6	4	Accepted
Emodin	-7.0	3	

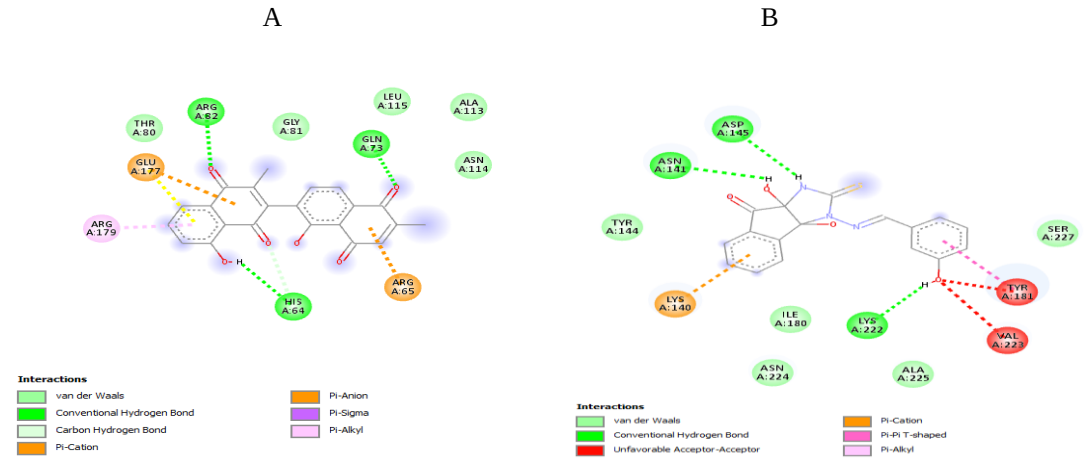

Figure 6: (**A**) shows the amino acids interactions between chitranone and Cyclophylin D (CypD). And (**B**) shows the amino acids interaction between Emodin and Cyclophylin D (CypD)

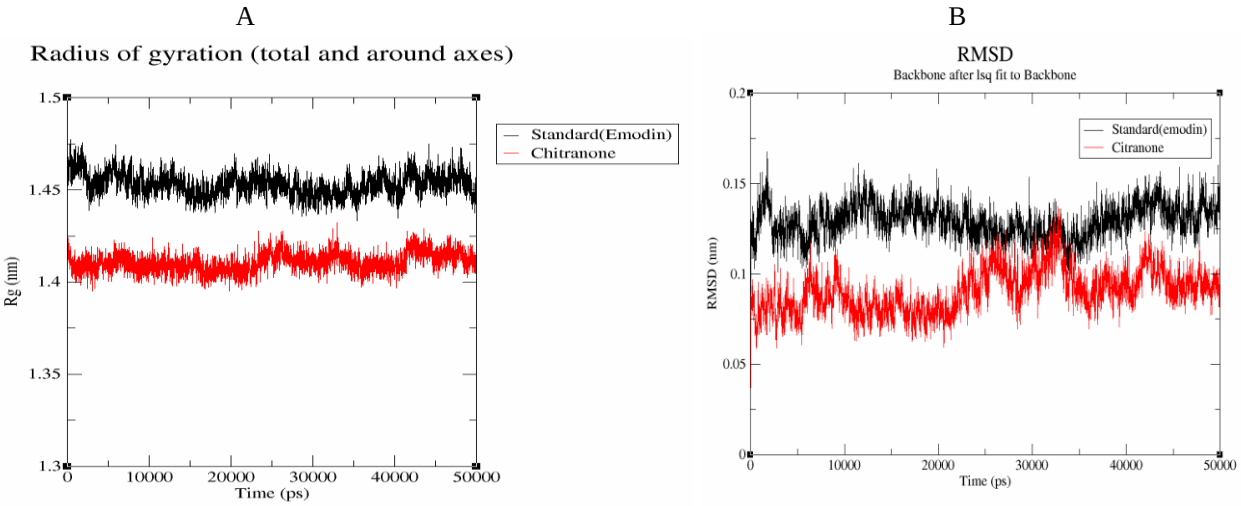

Figure 7: (**A**) shows the gyrate plot of the molecular dynamics simulation using GROMACS. A plot of Radius of Gyration (Rg) in nanometres (nm) against time in picoseconds (ps). The Gyration was observed 50000ps and (**B**) shows root mean square deviation (RSMD) plot of the molecular dynamics simulation using GROMACS. A plot of RSMD in nanometres (nm) against time in picoseconds (ps).

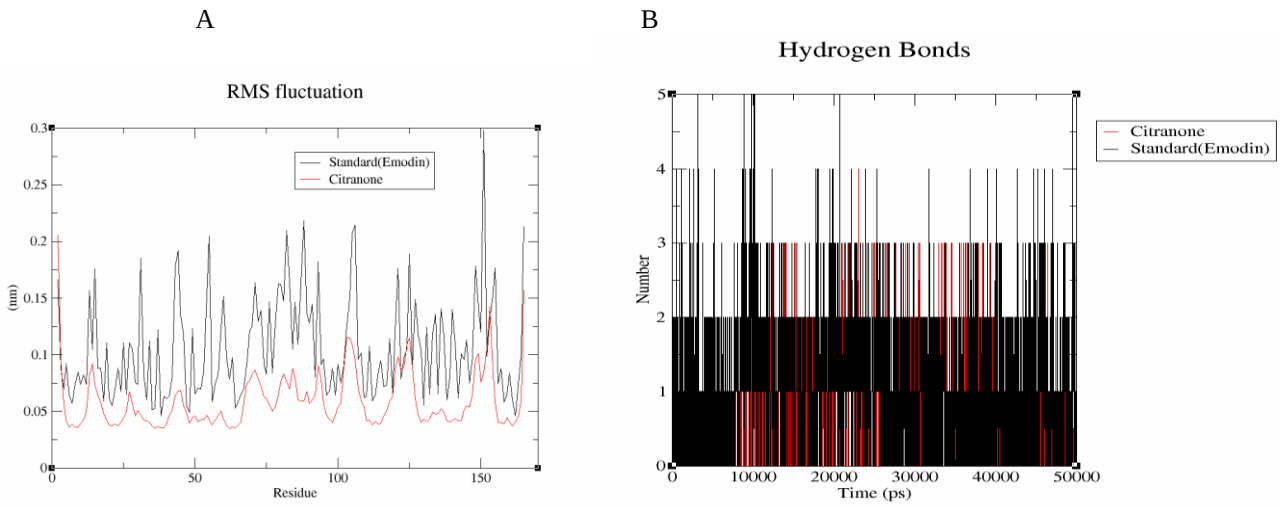

Figure 8: (**A**) shows root mean square fluctuation (RSMF) plot of the molecular dynamics simulation using GROMACS. A plot of RSMF in nanometres (nm) against Atom/Residue in grams (g). and (**B**) shows the average number of intermolecular H-bonds of Chitranone (lig.) and Emodin.

4. Discussion

Targeting mitochondria through apoptosis-inducing pathways remains a cornerstone of modern cancer therapy research (Chen *et al*., 2024). As central regulators of cell survival and death, mitochondria are critical in orchestrating the selective elimination of cancer cells. Previous investigations on botanical extracts have revealed that the root fraction of Plumbago zeylanica (PZ) is capable of inducing apoptosis, exhibiting cytotoxic effects even against multidrug-resistant (MDR) cancer cells, and activating the mitochondrial permeability transition (MPT) pore (Dalla *et al*., 2014). These findings support the growing body of evidence highlighting the therapeutic potential of plant-derived bioactive compounds as modulators of mitochondrial integrity.

The phytochemical screening of PZ demonstrated the presence of diverse classes of bioactive compounds, including alkaloids, anthraquinones, steroids, phenolic compounds, terpenoids, tannins, phlobatannins, saponins, glycosides, and proteins, consistent with earlier reports (Onen *et al*., 2021). These phytochemicals are widely recognized for their pharmacological significance, particularly in antimicrobial and anticancer therapies (Subhash *et al*., 2013). GC-FID and HPLC analyses further revealed plumbagin and chloroplumbagin as the major constituents with the highest peak values. These naphthoquinone derivatives are well documented for their antioxidant, anti-inflammatory, antimicrobial, anti-diabetic, and anticancer activities, and emerging studies have also pointed to their neuroprotective potential in neurodegenerative diseases such as Alzheimer's and Parkinson's (Ehigie *et al*., 2013).

Functional assays demonstrated that mPTP opening was significantly induced upon incubation of intact mitochondria with calcium across a range of concentrations (4–20 µg/mL). The ethyl acetate root fraction (ERF), n-hexane root fraction (HRF), aqueous root fraction (ARF), and butanol root fraction (BRF) all promoted pore opening, with fold increases ranging between 3.1 and 9.7 at increasing concentrations. Notably, the BRF induced the highest fold increase at 20 µg/mL (Fig. 3E), suggesting the presence of potent phytochemicals within this fraction capable of destabilizing mitochondrial integrity (Ehigie *et al*., 2013). The induction of mPTP opening aligns with established mechanisms wherein calcium overload, inorganic phosphate (Pi), and oxidative stress synergistically trigger pore opening, leading to mitochondrial swelling, outer membrane rupture, and subsequent release of pro-apoptotic factors such as cytochrome c and apoptosis-inducing factor (AIF) (Cong *et al*., 2024; Skulachev *et al*., 2023).

The observed increase in mitochondrial ATPase activity across groups treated with PZ root fractions (Fig. 4) provides additional evidence of mitochondrial dysfunction. Elevated ATPase activity accelerates ATP hydrolysis, which in turn reduces the availability of cellular energy reserves, thereby compromising key metabolic and physiological processes (Zahoor *et al*., 2020). This dysregulation of energy metabolism may contribute to apoptotic signaling, particularly in hepatocytes where energy balance is vital for cellular viability. Furthermore, decreased percentage inhibition of lipid peroxidation was observed in PZ-treated groups relative to control group. This decline suggests that the fractions enhance oxidative stress by impairing mitochondrial function, resulting in dissipation of membrane potential, increased electron leakage from the electron transport chain, and subsequent activation of the mPTP (Akhter *et al*., 2017). Such mitochondrial impairment is consistent with the known effects of phytochemicals that interfere with respiratory chain complexes, alter membrane permeability, and modulate redox balance (Clarke *et al*., 2013). Collectively, these events converge on the induction of apoptosis, underscoring the mechanistic role of PZ phytochemicals in cancer-related mitochondrial pathways.

Molecular docking studies provided further mechanistic insight by elucidating how specific phytochemicals interact with protein targets. Protein-ligand recognition is central to understanding substrate affinity and pharmacological potential (Sousa *et al*., 2006). In this study, phytochemicals from PZ demonstrated favorable drug-likeness properties based on physicochemical profiling. Of particular note, chitranone exhibited strong binding affinity, robust hydrogen bonding interactions, and compliance with Lipinski's rule of five, making it a promising candidate for further development. Subsequent molecular dynamics simulations revealed that chitranone maintained stable binding with the target protein, as confirmed by key parameters such as radius of gyration, root mean square deviation, root mean square fluctuation, and hydrogen bonding analysis. These results suggest that chitranone has the potential to modulate mitochondrial-related protein functions with structural stability, thereby validating its therapeutic promise (Khan *et al*., 2019).

The results of this study demonstrated that PZ root fractions exert significant effects on mitochondrial function, primarily through the induction of mPTP opening, modulation of ATPase activity, and enhancement of oxidative stress pathways. The presence of bioactive compounds such as plumbagin, chloroplumbagin, and chitranone underscores their pharmacological relevance as apoptosis-inducing agents. These findings not only reinforce the role of PZ as a promising natural source of anticancer compounds but also highlight the importance of mitochondrial targeting as a therapeutic strategy for cancer management.

5. Conclusion

The initiation of mitochondrial permeability transition pore (mPTP) opening and increase in ATPase activity, are positive indications of the fractions' ability to induce apoptosis, leading to cell death and inhibition of cancer growth. Our integrated *in vitro* and *in silico* study reveals a potential link between *PZ* fractions and mitochondrial dysfunction, indicating that these fractions may initiate a cascade of oxidative stress in male Wistar rat. This finding has significant implications for our understanding of fraction's biological effects and highlights the need for further research into its potential impact on cellular health. *In silico* studies revealed the binding mechanism of Chitranone, a phytochemical from *PZ*, to Cyclophilin D, a crucial regulator of mPTP opening, offering

valuable insights into apoptosis mechanisms and paving the way for innovative therapeutic approaches.

Conflict of Interest

Authors declared no conflicts of interest.

References

Agbaje, E., & Adeniran, J. (2009a). Some Gastrointestinal Effects of the Aqueous Root Fraction of *Plumbago zeylanica* (Lead Wort). *African Journal of Biomedical Research*, *12*(1), 63–68.

Agbaje, E., & Adeniran, J. (2009b). Some Gastrointestinal Effects of the Aqueous Root Fraction of *Plumbago zeylanica* (Lead Wort). *African Journal of Biomedical Research*, *12*(1), 63–68.

Bonora, M., Missiroli, S., Perrone, M., Fiorica, F., Pinton, P., & Giorgi, C. (2021). Mitochondrial control of genomic instability in cancer. *Cancers*, *13*(8), 1914.

Chauhan, M. (2014). A review on Morphology, Phytochemistry and Pharmacological activities of medicinal herb *Plumbago zeylanica* Linn. *Journal of Pharmacognosy and Phytochemistry*, *3*(2), 95–118.

Chen, Z., Chen, L., dong Lyu, T., Weng, S., Xie, Y., Jin, Y., Wu, O., Jones, M., Kwan, K., & Makvnadi, P. (2024). Targeted mitochondrial nanomaterials in biomedicine: Advances in therapeutic strategies and imaging modalities. *Acta Biomaterialia*.

Clarke, K. J., & Porter, R. K. (2013). Uncoupling protein 1 dependent reactive oxygen species production by thymus mitochondria. *The International Journal of Biochemistry & Cell Biology*, *45*(1), 81–89.

Dalla Via, L., N. Garcia-Argaez, A., Martinez-Vazquez, M., Grancara, S., Martinis, P., & Toninello, A. (2014). Mitochondrial permeability transition as target of anticancer drugs. *Current Pharmaceutical Design*, *20*(2), 223–244.

Guguloth, S. K., Malothu, N., Ganta, N. M., Ramakrishna, K., & Guntupalli, C. (2023). Antiplatelet and antithrombotic properties of methanolic leaf fraction of *Plumbago zeylanica* L.: GC-MS and HR-LCMS metabolite profiling. *South African Journal of Botany*, *159*, 627–634.

Gupta, V. B., Chitranshi, N., den Haan, J., Mirzaei, M., You, Y., Lim, J. K., Basavarajappa, D., Godinez, A., Di Angelantonio, S., & Sachdev, P. (2021). Retinal changes in Alzheimer's disease—Integrated prospects of imaging, functional and molecular advances. *Progress in Retinal and Eye Research*, *82*, 100899.

Halestrap, A. P. (2009a). What is the mitochondrial permeability transition pore? *Journal of Molecular and Cellular Cardiology*, *46*(6), 821–831.

Halestrap, A. P. (2009b). What is the mitochondrial permeability transition pore? *Journal of Molecular and Cellular Cardiology*, *46*(6), 821–831.

Ittiyavirah, S. P., & Ruby, R. (2014). Effect of hydro-alcoholic root extract of *Plumbago zeylanica* l alone and its combination with aqueous leaf extract of *Camellia sinensis* on haloperidol induced parkinsonism in wistar rats. *Annals of neurosciences*, 21(2), 47–50.

Khan, R., Plahras, J., Johnston, B. C., Scaffidi, M. A., Grover, S. C., & Walsh, C. M. (2019). Virtual reality simulation training in endoscopy: A Cochrane review and meta-analysis. *Endoscopy*, *51*(07), 653–664.

Lardy, H. A., & Wellman, H. (1953). The catalytic effect of 2, 4-dinitrophenol on adenosinetriphosphate hydrolysis by cell particles and soluble enzymes. *Journal of Biological Chemistry*, *201*(1), 357–370.

Onen, M., Emond, N., Li, J., Yildiz, B., & Del Alamo, J. A. (2021). CMOS-compatible protonic programmable resistor based on phosphosilicate glass electrolyte for analog deep learning. *Nano Letters*, *21*(14), 6111–6116.

Rajabi, H., Mosleh, M. H., Mandal, P., Lea-Langton, A., & Sedighi, M. (2021). Sorption behaviour of xylene isomers on biochar from a range of feedstock. *Chemosphere*, *268*, 129310.

Ruberto, G., Baratta, M. T., Deans, S. G., & Dorman, H. J. (2000). Antioxidant and antimicrobial activity of *Foeniculum vulgare* and *Crithmum maritimum* essential oils. *Planta medica*, 66(8), 687–693.

Sauter, T., Arndt, A., & Schneider, C. (2020a). COSIPY v1. 3–an open-source coupled snowpack and ice surface energy and mass balance model. *Geoscientific Model Development*, *13*(11), 5645–5662.

Sauter, T., Arndt, A., & Schneider, C. (2020b). COSIPY v1. 3–an open-source coupled snowpack and ice surface energy and mass balance model. *Geoscientific Model Development*, *13*(11), 5645–5662.

Sharifi-Rad, J., Ozleyen, A., Boyunegmez Tumer, T., Oluwaseun Adetunji, C., El Omari, N., Balahbib, A., Taheri, Y., Bouyahya, A., Martorell, M., & Martins, N. (2019a). Natural products and synthetic analogs as a source of antitumor drugs. *Biomolecules*, *9*(11), 679.

Sharifi-Rad, J., Ozleyen, A., Boyunegmez Tumer, T., Oluwaseun Adetunji, C., El Omari, N., Balahbib, A., Taheri, Y., Bouyahya, A., Martorell, M., & Martins, N. (2019b). Natural products and synthetic analogs as a source of antitumor drugs. *Biomolecules*, *9*(11), 679.

Shukla, B., Saxena, S., Usmani, S., & Kushwaha, P. (2021a). Phytochemistry and pharmacological studies of *Plumbago zeylanica* L.: A medicinal plant review. *Clinical Phytoscience*, *7*, 1–11.

Shukla, B., Saxena, S., Usmani, S., & Kushwaha, P. (2021b). Phytochemistry and pharmacological studies of *Plumbago zeylanica* L.: A medicinal plant review. *Clinical Phytoscience*, *7*, 1–11.

Skulachev, V. P. (1996). Why are mitochondria involved in apoptosis? Permeability transition pores and apoptosis as selective mechanisms to eliminate superoxide-producing mitochondria and cell. *FEBS Letters*, *397*(1), 7–10.

Skulachev, V., Vyssokikh, M. Y., Chernyak, B., Averina, O., Andreev-Andrievskiy, A., Zinovkin, R., Lyamzaev, K., Marey, M., Egorov, M., & Frolova, O. (2023). Mitochondrion-targeted antioxidant SkQ1 prevents rapid animal death caused by highly diverse shocks. *Scientific Reports*, *13*(1), 4326.

Sousa, S. F., Fernandes, P. A., & Ramos, M. J. (2006). Protein–ligand docking: Current status and future challenges. *Proteins: Structure, Function, and Bioinformatics*, *65*(1), 15–26.

Subhash, N. V. (2013). *To Evaluate the Frequency of Kirsten-Ras Gene Mutation and Its Association with Clinical and Pathological Factors in* Colour*ectal Adenocarcinoma*.

Verma, M., Lizama, B. N., & Chu, C. T. (2022). Excitotoxicity, calcium and mitochondria: a triad in synaptic neurodegeneration. Translational neurodegeneration, 11(1), 3.

Wacquier, B., Combettes, L., & Dupont, G. (2020). Dual dynamics of mitochondrial permeability transition pore opening. *Scientific Reports*, *10*(1), 3924.

Wang, M., Liu, Y., Liang, Y., Naruse, K., & Takahashi, K. (2021). Systematic understanding of pathophysiological mechanisms of oxidative stress-related conditions—diabetes mellitus, cardiovascular diseases, and ischemia–reperfusion injury. Frontiers in cardiovascular medicine, 8, 649785.

Zahoor, A., Messerschmidt, K., Boecker, S., & Klamt, S. (2020). ATPase-based implementation of enforced ATP wasting in Saccharomyces cerevisiae for improved ethanol production. *Biotechnology for Biofuels*, *13*, 1–12.

Zou, W. (2024). Mechanism and treatment of intracerebral hemorrhage focus on mitochondrial permeability transition pore. *Frontiers in Molecular Neuroscience*, *17*, 1423132.

•*Thank you for publishing with us.*